Title
Hemoglobin contrast in magnetomotive optical Doppler tomography.

Journal
Optics Letters, 31(6)

ISSN
0146-9592

Authors
Kim, Jeehyun
Oh, Junghwan
Milner, Thomas E
et al.

Publication Date
2006-03-15

DOI
10.1364/ol.31.000778

Hemoglobin contrast in magnetomotive optical Doppler tomography

Jeehyun Kim

Beckman Laser Institute and Medical Clinic, University of California at Irvine, 1002 Health Sciences Road East, Irvine, California 92612

Junghwan Oh and Thomas E. Milner

Department of Biomedical Engineering, University of Texas at Austin, Austin, Texas 78712

J. Stuart Nelson

Beckman Laser Institute and Medical Clinic, University of California at Irvine, 1002 Health Sciences Road East, Irvine, California 92612

Received November 2, 2005

We introduce a novel contrast mechanism for imaging blood flow by use of magnetomotive optical Doppler tomography (MM-ODT), which combines an externally applied temporally oscillating high-strength magnetic field with ODT to detect erythrocytes moving according to the field gradient. Hemoglobin contrast was demonstrated in a capillary tube filled with moving blood by imaging the Doppler frequency shift, which was observed independently of blood flow rate and direction. Results suggest that MM-ODT may be a promising technique with which to image blood flow. © 2006 Optical Society of America

OCIS codes: 170.4500, 170.3880, 160.3820, 290.5850.

Optical coherence tomography (OCT) uses the short temporal coherence properties of broadband light to extract structural information from heterogeneous samples such as biological tissue. The ability to locate the microvasculature precisely is important for diagnostics and treatments that require characterization of blood flow. Recently several efforts to introduce novel blood flow contrast mechanisms, including protein microspheres incorporating nanoparticles into their shells,[1] plasmon-resonant gold nanoshells,[2] and use of magnetically susceptible micrometer-sized particles with an externally applied magnetic field,[3] have been reported.

A high iron content, which is due to the presence of four atoms in each hemoglobin molecule, and the high concentration of hemoglobin in human red blood cells (RBCs) make this molecule a useful test case for investigating magnetomotive effects on endogenous magnetically susceptible particles in biologic tissue.[4] A RBC suspended in plasma and placed in a magnetic field gradient experiences forces and torques that tend to position and align it with respect to the field's direction. The magnetic force, in the direction of probing light z, is given by

$$F_z = \frac{\Delta\chi V}{\mu_0} B \frac{\partial B}{\partial z}, \tag{1}$$

where V is the particle volume, μ_0 is the permeability of free space, B is the magnitude of the magnetic flux density along the z axis, and $\Delta\chi$ is the difference between the susceptibilities of the RBC and of the surrounding plasma to the force, which gives a dynamic RBC displacement $[z(t)]$ that can be included in the analytic OCT fringe expression, I_f:

$$I_f \propto 2\sqrt{I_R I_S} \exp\left\{ i\left[2\pi f_0 t + \frac{4\pi n z(t)}{\lambda_0} \right] \right\}, \tag{2}$$

where I_R and I_S are the backscattered intensities from the reference and the sample arms, respectively, f_0 is the fringe carrier frequency, λ_0 is the light source's center wavelength, n is the medium's refractive index, and $z(t)$ is the dynamic RBC displacement.

We present a novel extension of magnetomotive OCT that is analogous to the features of functional MRI to image hemoglobin in blood erythrocytes. The contrast of optical Doppler tomography (ODT) images can be enhanced by activation of iron-containing hemoglobin molecules in blood with an externally applied high-strength magnetic field gradient. Importantly, our approach requires no exogenous contrast agent to detect blood flow and location.

Herein, we describe magnetomotive optical Doppler tomography (MM-ODT) imaging of the Doppler shift of hemoglobin by applying an oscillating magnetic field to moving blood. The ODT light source consisted of a superluminescent diode (Model BWC-SLD-1C, B&W TEK, Inc., Newark, Deleware) centered at 1.3 μm. A rapid-scanning optical delay line was used in the reference arm and was aligned such that no phase modulation was generated when the group phase delay was scanned at 4 kHz. The phase modulation was generated by an electro-optic waveguide phase modulator that produced a single carrier frequency (1 MHz). A hardware in-phase and in-quadrature demodulator with high-bandpass filters was constructed to improve imaging speed. Doppler information was calculated with the Kasai autocorrelation velocity estimator.[5] A 750 μm inner-diameter glass capillary tube was placed

0146-9592/06/060778-3/$15.00

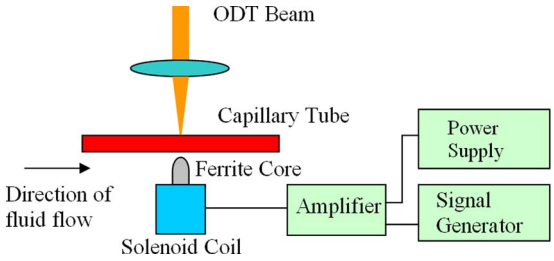

Fig. 1. (Color online) Schematic diagram of the probe beam, the flow sample, and the solenoid coil.

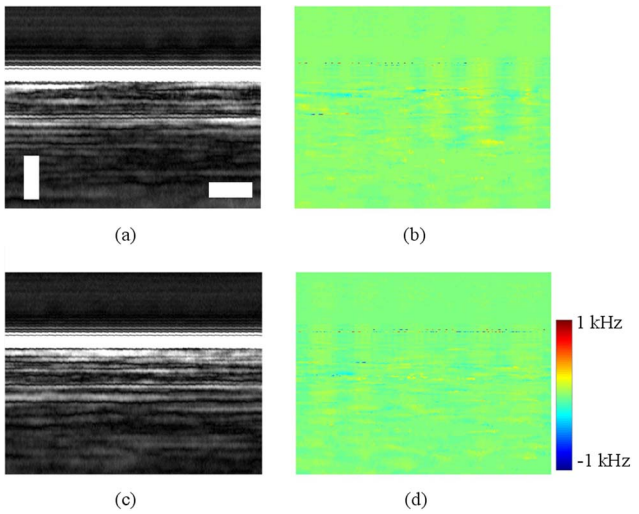

Fig. 2. (Color online) (a), (b) OCT and ODT *M*-mode images, respectively, without an external magnetic field. (c), (d) OCT and ODT images, respectively, with a 50 Hz magnetic field. White vertical bar, 200 μm; white horizontal bar, 20 ms.

perpendicularly to the probing beam. Fluids used for flow studies were injected through the tube at a constant flow rate controlled by a dual-syringe pump (Harvard Apparatus 11 Plus, Holliston, Mass.). A solenoid coil (Ledex 4EF) with a cone-shaped ferrite core at the center (Fig. 1) and driven by a current amplifier supplying as much as 960 W of power was placed underneath the sample during MM-ODT imaging. The combination of the core and solenoid by high-power operation dramatically increased the magnetic field strength ($B_{\max}=0.7$ T) at the tip of the core and also focused the magnetic force on the targeted samples. The magnetic force applied to the capillary tube was varied by the sinusoidal current to induce RBC movement.

To demonstrate the MM-ODT approach we recorded *M*-mode OCT–ODT images of a capillary glass tube filled with a stationary low-susceptibility turbid solution with and without an external magnetic field as a control sample. The low-susceptibility turbid solution was a mixture of deionized water and 0.5 μm latex microspheres ($\mu_s=5$ mm^{-1}). The magnetic flux density and its frequency were approximately 0.7 T and 50 Hz, respectively. The field gradient ($\partial B/\partial z$) in the optical measurement zone was measured (220 T/m) with a magnetometer over a 1 mm line segment extending from the tip along the axis of the ferrite core. *M*-mode OCT–ODT images were acquired at a rate of 100 ms per frame. Figures 2(a) and 2(b) show *M*-mode OCT and ODT images without any external magnetic field. The ODT image [Fig. 2(b)] contains small random phase fluctuations that are due to ambient vibration through the optical path. Figures 2(c) and 2(d) show *M*-mode OCT–ODT images with a 50 Hz externally applied magnetic field. No distinguishable Doppler shift could be observed in the ODT image [Fig. 2(d)], indicating no interaction between the external magnetic field and the moving latex microspheres.

Deoxygenated blood was extracted from the vein of a male volunteer's left arm and diluted with saline. During preparation, blood was not exposed directly to air, so the sample remained deoxygenated. To simulate flow, we injected blood through the capillary tube by using a syringe pump at a constant flow rate. As Fig. 3 shows, the oscillating Doppler frequency shift that results from RBC movement could be observed at two flow rates (5 and 30 mm/s). Because the flow direction was nearly perpendicular to the probe beam, no significant Doppler frequency shift was distinguishable at the 5 mm/s flow rate [Fig. 3(a)] without any external magnetic field. In the case of the 30 mm/s high blood flow rate, as shown in Fig. 3(c), the Doppler frequency shift caused by the flow could be observed. For maximum contrast enhancement, the probe beam should be directed parallel to the gradient of the magnetic field's strength. Application of a 50 Hz magnetic field increased the Doppler contrast of blood at both slow and fast flow rates, as shown in Figs. 3(b) and 3(d). Note that in the 30 mm/s high-flow-rate image, higher contrast is observed than with the low-flow-rate image but that the Doppler frequency shift of the former as a function of depth is less homogeneous than the latter, which is indicative of perturbation by blood flow. The same blood was diluted to 5% hematocrit, but no RBC movement could be observed below 8% hematocrit. We calculated Doppler frequency shift profiles from the ODT images by averaging 20 lines indicated by horizontal arrows in Figs. 3(a) and 3(b). Figure 4(a) indicates no signifi-

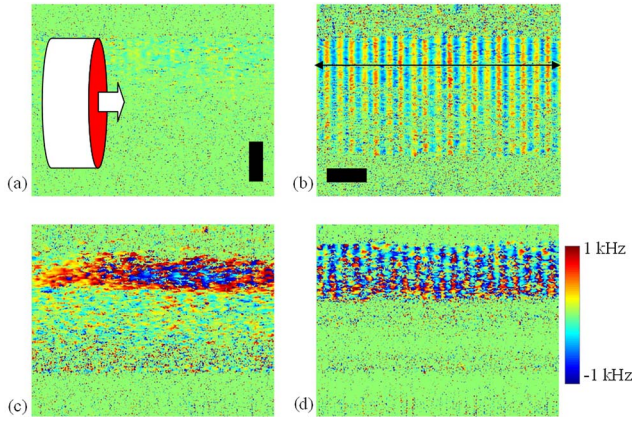

Fig. 3. (Color online) (a), (b) *M*-mode ODT images of 5 mm/s blood flow without and with a 50 Hz magnetic field, respectively. (c), (d) *M*-mode ODT images of 30 mm/s blood flow without and with a 50 Hz magnetic field, respectively. Black vertical bar, 200 μm; black horizontal bar, 20 ms.

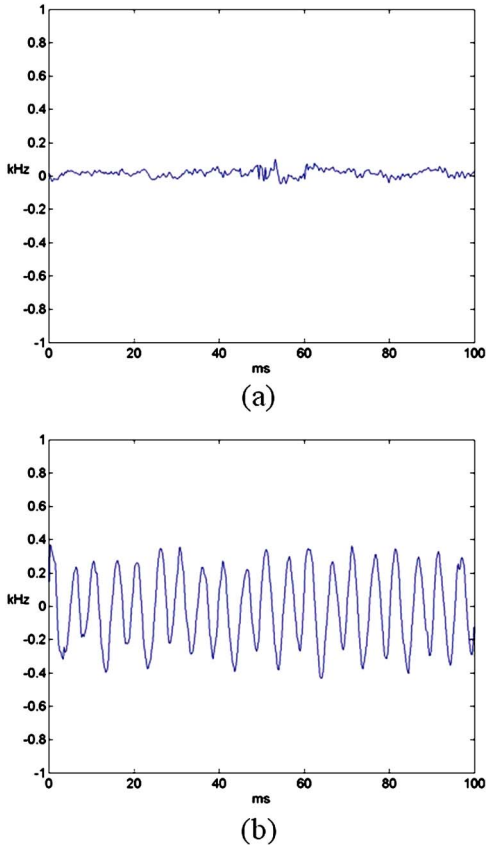

Fig. 4. (Color online) Doppler frequency shift profiles (a) without an external magnetic field and (b) with a 50 Hz magnetic field.

cant Doppler frequency shift over a 100 ms observation period, whereas Fig. 4(b) displays ±200 to 300 Hz Doppler frequency shifts oscillating 20 times over 100 ms (200 Hz).

RBCs under the influence of a strong magnetic-field gradient tend to travel either toward or away from the field source, depending on whether their magnetic properties are paramagnetic or diamagnetic.[4] RBCs moving toward the probe are colored red (Fig. 3), while blue indicates RBC movement in the opposite direction. When only a magnetic force is present (recoil and pressure-gradient forces are absent or neglected), direct integration of Eq. (1) gives $z(t)=\epsilon(t)+z_0\cos(4\pi f_m t)$, where $\epsilon(t)=a_0t^2$, a_0 and z_0 are constants and are dependent on χ, V, and B, and f_m is the modulation frequency of the magnetic flux density. Because $\epsilon(t)$ is proportional to time squared, the displacement is strongly dominant in one direction in free space, and the RBC oscillation may not be visible. However, as the local concentration of RBCs increases in the capillary tube in response to an external magnetic field, osmotic and elastic recoil forces increase and hinder further RBC movement into the field. Equivalently, forces driving RBCs find an equilibrium state at which the magnetic force is balanced by the sum of the recoil forces. In a confined system such as a blood vessel, $\epsilon(t)$ becomes negligible at sufficiently long times (in a few seconds) because recoil and drag forces impede the free-space acceleration of the RBCs related to $\epsilon(t)$. Once these forces balance, free-space acceleration of the RBCs approaches zero and the sinusoidal variation of the magnetic force dominates RBC displacement. Sinusoidal variation of the RBC displacement $[z(t)=z_0\cos(4\pi f_m t)]$ produced harmonics in the interference fringe intensity (I_f) according to relation (2). Because of the coherent detection scheme employed in our experiments, the harmonics remain centered at 0 Hz, even after demodulation. According to Eq. (1) the magnetic-force frequency is two times the magnetic field frequency (f_m). In our experiments f_m was set to give a value of I_f consisting primarily of the $4f_m$ harmonic [Fig. 4(b)], whereas the fundamental frequency (the magnetic-force frequency) of the RBC displacement is $2f_m$. Because the magnetic susceptibility of hemoglobin is dependent on oxygen saturation, RBC displacement *in vivo* may differ from that reported herein and will require further study.

In conclusion, we have demonstrated what is believed to be the first implementation of MM-ODT for improved Doppler imaging of blood flow by use of an external oscillating magnetic field. Mechanical movement of RBCs in blood flow was introduced by a temporally oscillating high-strength magnetic field. The controlled and increased Doppler frequency in MM-ODT may provide a new investigational tool with which to study blood transport.

This research was supported by research grants from the National Institutes of Health (AR47551, EBOO2495, and EB002021) and from the Texas Advanced Technology Program. J. Kim's email address is jeehk@uci.edu.

References

1. T. M. Lee, O. L. Oldenburg, S. Sitafalwalla, D. L. Marks, W. Luo, F. J. J. Toublan, K. S. Suslick, and S. A. Boppart, Opt. Lett. **28**, 1546 (2003).
2. C. Loo, A. Lin, L. Hirsch, M. H. Lee, J. Barton, N. Halas, J. West, and R. Drezek, Technol. Cancer Res. Treat. **3**, 33 (2004).
3. A. L. Oldenburg, J. R. Gunther, and S. A. Boppart, Opt. Lett. **30**, 747 (2005).
4. M. Okazaki, N. Maeda, and T. Shiga, Eur. Biophys. J. **14**, 139 (1987).
5. V. X. D. Yang, M. L. Gordon, B. Qi, J. Pekar, S. Lo, E. Seng-Yue, A. Mok, B. C. Wilson, and I. A. Vitkin, Opt. Express **11**, 794 (2003).